geoconvention
Calgary • Canada • May 7-11 2018

Time-domain elastic Gauss-Newton full-waveform inversion via matrix-free adjoint-state method

Ke Chen and Mauricio D. Sacchi, Department of Physics, University of Alberta

Summary

A time-domain matrix-free elastic Gauss-Newton FWI algorithm is formulated based on elastic least-squares reverse time migration (LSRTM) algorithm. The proposed algorithm consists of two loops of iterations: the outer Gauss-Newton nonlinear iterations and the inner conjugate gradient least-squares (CGLS) linear iterations. The Gauss-Newton search direction in each outer FWI iteration is computed using the matrix-free CGLS algorithm. This step is equivalent to apply an elastic LSRTM on data residuals. The CGLS algorithm can be safely used for solving the Gauss-Newton search direction because our discretized numerical versions of elastic Born and RTM operators passed the dot-product test. We use the proposed algorithm to simultaneously invert for P- and S-wave velocities. The density is assumed to be known. The proposed elastic Gauss-Newton FWI generates an improvement on the inverted models when compared to the nonlinear conjugate gradient method based elastic FWI.

Introduction

Full-waveform inversion (FWI) (Tarantola, 1986) aims at estimating subsurface model parameters using the full-wave mode data recorded by seismic receivers. Mora (1987) numerically studies the 2D time-domain elastic FWI of synthetic reflection and transmission multicomponent data. Kohn et al. (2012) investigate the influence of model parameterization in 2D time-domain elastic full-waveform inversion. In this paper, we propose a time-domain matrix-free elastic Gauss-Newton FWI algorithm based on elastic LSRTM algorithm (Chen and Sacchi, 2017a,b). The proposed algorithm consists of two loops of iterations: the outer Gauss-Newton nonlinear iterations and the inner CGLS linear iterations (Paige and Saunders, 1982). The Gauss-Newton search direction is computed using the CGLS algorithm. We recognize that this step is equivalent to apply an elastic LSRTM on data residuals (Chen and Sacchi, 2017b). The CGLS algorithm can be safely used for solving the Gauss-Newton search direction because our discretized numerical versions of elastic Born and RTM operators passed the dot-product test (Claerbout, 1992). The inner CGLS linear iterations are preconditioned using the elastic pseudo-Hessian operator (Chen and Sacchi, 2017b). Our algorithm is matrix-free, in other words, it only requires the forward Jacobian and adjoint Jacobian operator applied "on the fly" to vectors. The operators are applied on vectors efficiently via the adjoint-state method (Lions, 1971). We simultaneously invert for P- and S-wave velocities. The proposed elastic Gauss-Newton FWI generates better inverted models than the nonlinear conjugate gradient method based elastic FWI. Time-domain elastic Gauss-Newton FWI has also been investigated in Sheen et al. (2006) and Epanomeritakis et al. (2008). However, both papers do not consider the multiparameter crosstalk problem. Epanomeritakis et al. (2008) only inverts for the shear modulus. In Sheen et al. (2006), the Jacobian matrix and Hessian matrix are explicitly computed using reciprocity, which is too expensive for large-scale problems. Recently, Pan et al. (2016) discuss the Gauss-Newton and full-Newton method in elastic HTI media. However, it is also based on explicitly computing and inverting the Hessian which impedes its application to large-scale problems.

Theory

We assume a heterogeneous, isotropic elastic earth media. The elastic wave equation can be abstractly written as

$$\mathscr{S}(\mathbf{m})\mathbf{u} = \mathbf{f}, \tag{1}$$

where $\mathbf{u} = (v_x, v_z, \sigma_{xx}, \sigma_{zz}, \sigma_{xz})^T$ is the wavefield vector, $\mathbf{f} = (0, 0, f_{xx}, f_{zz}, 0)^T$ is the source vector, $\mathscr{S}(\mathbf{m})$ is the wave equation operator, and $\mathbf{m}$ denotes the model parameter vector. FWI is usually formulated as a nonlinear least-squares inverse problem that minimizes the functional (Tarantola, 1984)

$$\mathscr{J}(\mathbf{m}) = \frac{1}{2}\sum_{i=1}^{N_s} \|\mathbf{d}_i(\mathbf{m}) - \mathbf{d}_i^{obs}\|_2^2, \tag{2}$$

where $\mathbf{d}_i(\mathbf{m}) = \mathscr{T}\mathbf{u}_i(\mathbf{m})$ is the forward modeled seismic data for ith shot, $\mathscr{T}$ is the sampling operator, $\mathbf{d}_i^{obs}$ is the observed seismic data for ith shot, and $\|\cdot\|_2$ denotes the ℓ_2 norm of vector. The elastic Gauss-Newton FWI iteratively updates the model

$$\mathbf{m}^{(k+1)} = \mathbf{m}^{(k)} + \eta^{(k)}\delta\mathbf{m}^{(k)} = \mathbf{m}^{(k)} - \eta^{(k)}{\mathbf{H}_a^{(k)}}^{-1}\mathbf{g}^{(k)}, \tag{3}$$

where $\mathbf{m}^{(k)}$ is the model at kth iteration, $\eta^{(k)}$ is the step size, $\delta\mathbf{m}^{(k)}$ is the Gauss-Newton search direction, $\mathbf{H}_a^{(k)}$ is the approximated Hessian and $\mathbf{g}^{(k)}$ is the gradient. The gradient can be expressed as

$$\mathbf{g} = \frac{\partial\,\mathscr{J}(\mathbf{m})}{\partial\mathbf{m}} = \sum_{i=1}^{N_s}\left(\frac{\partial\mathbf{d}_i}{\partial\mathbf{m}}\right)^{\dagger}\left(\mathbf{d}_i - \mathbf{d}_i^{obs}\right) = \sum_{i=1}^{N_s}\mathbf{L}_i^{\dagger}(\mathbf{d}_i - \mathbf{d}_i^{obs}), \tag{4}$$

where $\mathbf{L}_i = \partial\mathbf{d}_i/\partial\mathbf{m}$ denotes the elastic Born operator, $\mathbf{L}_i^{\dagger} = (\partial\mathbf{d}_i/\partial\mathbf{m})^{\dagger}$ denotes the elastic RTM operator. The Gauss-Newton Hessian operator can be expressed as

$$\mathbf{H}_a = \sum_{i=1}^{N_s}\left(\frac{\partial\mathbf{d}_i}{\partial\mathbf{m}}\right)^{\dagger}\left(\frac{\partial\mathbf{d}_i}{\partial\mathbf{m}}\right) = \sum_{i=1}^{N_s}\mathbf{L}_i^{\dagger}\mathbf{L}_i. \tag{5}$$

Directly solving the Gauss-Newton step $\delta\mathbf{m} = -\mathbf{H}_a^{-1}\mathbf{g}$ is prohibitively expensive. Instead, we solve the following linear system of equations

$$\mathbf{H}_a\delta\mathbf{m} = -\mathbf{g} \tag{6}$$

or equivalent

$$\sum_{i=1}^{N_s}\mathbf{L}_i^{\dagger}\mathbf{L}_i\delta\mathbf{m} = \sum_{i=1}^{N_s}\mathbf{L}_i^{\dagger}\delta\mathbf{d}_i, \tag{7}$$

where $\delta\mathbf{d}_i = \mathbf{d}_i^{obs} - \mathbf{d}_i$ is the data residual. Solving equation 7 is equivalent to solving the least-squares minimization problem

$$\mathscr{J}_{gn}(\delta\mathbf{m}) = \frac{1}{2}\sum_{i=1}^{N_s}\|\mathbf{L}_i\delta\mathbf{m} - \delta\mathbf{d}_i\|_2^2. \tag{8}$$

We recognize that the above least-squares minimization problem is actually equivalent to solving an elastic LSRTM problem on data residuals (Chen and Sacchi, 2017b). We carefully discretize the two operators $\mathbf{L}_i$ and $\mathbf{L}_i^{\dagger}$ to make sure that they pass the dot-product test. This allows us to use the conjugate gradient least-squares (CGLS) algorithm to solve equation 8. We also adopted the pseudo-Hessian to precondition the linear system of equations for acceleration (Shin et al., 2001). The proposed time-domain matrix-free elastic Gauss-Newton FWI algorithm is summarized in algorithm 1.

Algorithm 1 Time-domain matrix-free elastic Gauss-Newton FWI

Initialize: $\mathbf{m}^{(0)}$
for $k = 0, 1, \cdots$ **while** not converge **do**
1. Forward modeling: $\mathbf{d}_i^{(k)} = \mathbf{d}_i(\mathbf{m}^{(k)})$
2. Compute data residual: $\delta\mathbf{d}_i^{(k)} = \mathbf{d}_i^{obs} - \mathbf{d}_i^{(k)}$
3. Compute Gauss-Newton search direction $\delta\mathbf{m}^{(k)}$ by solving

$$\min_{\delta\mathbf{m}^{(k)}} \frac{1}{2}\sum_{i=1}^{N_s}\|\mathbf{L}_i^{(k)}\delta\mathbf{m}^{(k)} - \delta\mathbf{d}_i^{(k)}\|_2^2$$

   using preconditioned CGLS algorithm.
4. Compute step size $\eta^{(k)}$ via parabola fitting.
5. $\mathbf{m}^{(k+1)} = \mathbf{m}^{(k)} + \eta^{(k)}\delta\mathbf{m}^{(k)}$

end

Examples

The codes for our numerical examples were written in C and parallelized with Message Passing Interface (MPI) over shots. In this acticle, we simultaneously invert for P- and S- wave velocities and assume that the density is known. We compare the results of conventional elastic FWI based on nonlinear conjugate gradient method (hereafter, we call it elastic NLCG FWI for short) and the proposed elastic Gauss-Newton FWI method. For both methods, we adopt the multiscale approach (Bunks et al., 1995).

Figure 1 a and d show the true P- and S-wave velocity models for the elastic inclusion model. The velocity anomalies for P and S are in different positions. Figure 1 g and h show the starting P- and S-wave velocity models that contain two layers without of the velocity anomalies. The results of elastic NLCG FWI are shown in Figure 1 b and e. These results were computed after 20 nonlinear conjugate gradient iterations. The elastic NLCG FWI recovered the main features of the velocity anomalies. However, there are artifacts in the inverted models. Most important, there is some crosstalk between the inverted P-wave and S-wave velocity models. The elastic Gauss-Newton FWI has iterated 10 times for the outer FWI loop and 20 times for the inner CGLS loop (Figure 1 c and f). The velocity models computed with elastic Gauss-Newton FWI are better resolved than the models computed with elastic NLCG FWI. The artifacts and crosstalk are reduced by elastic Gauss-Newton FWI in comparison to the elastic NLCG FWI.

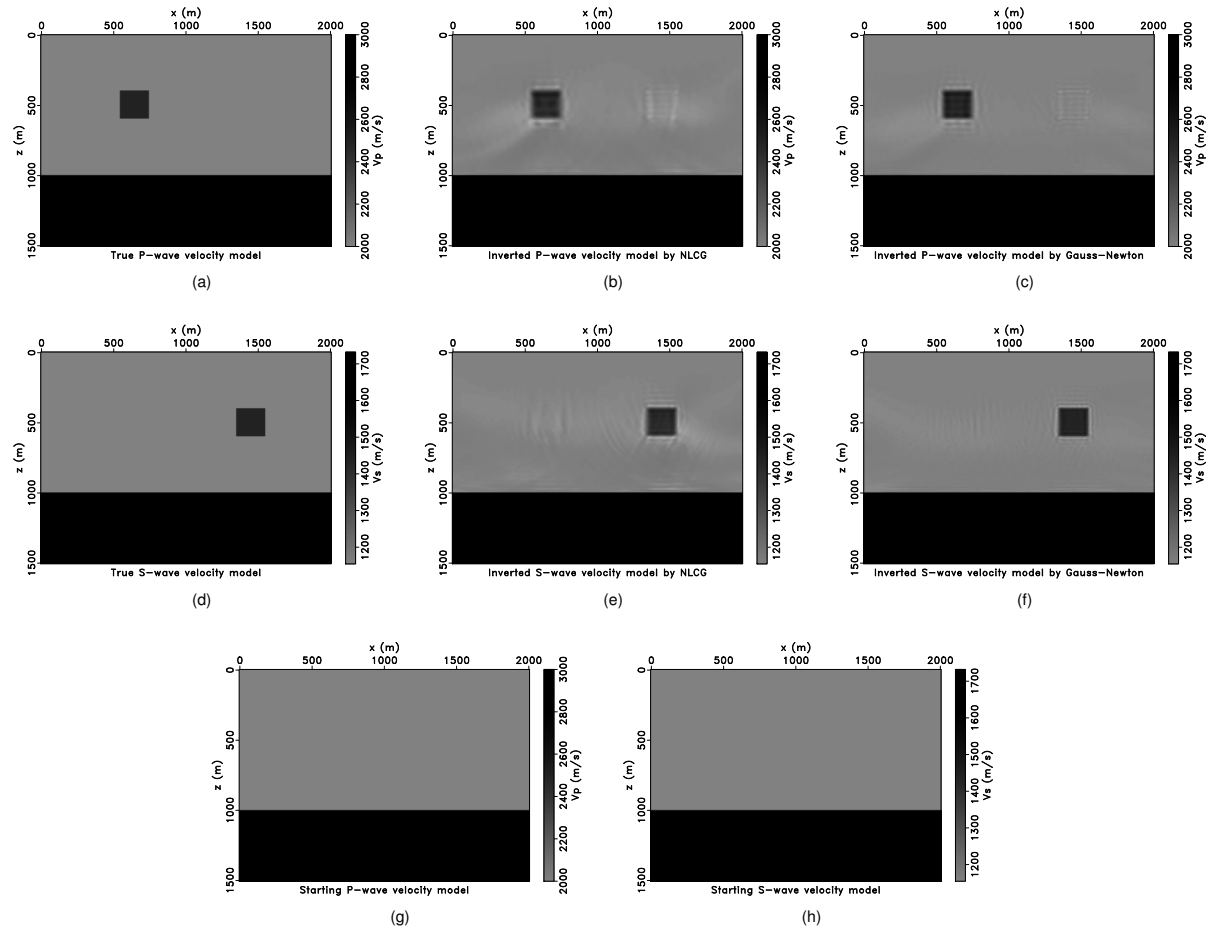

Figure 1: Elastic inclusion model. (a) True P-wave velocity model. (b) Inverted P-wave velocity model by elastic NLCG FWI. (c) Inverted P-wave velocity model by elastic Gauss-Newton FWI. (d) True S-wave velocity model. (e) Inverted S-wave velocity model by elastic NLCG FWI. (f) Inverted S-wave velocity model by elastic Gauss-Newton FWI. (g) Starting P-wave velocity model. (h) Starting S-wave velocity model.

Figure 2 a and d show the true P- and S-wave velocity models for the elastic Marmousi2 model. The P- and S-wave velocity models are uncorrelated. Figure 2 g and h show the starting P- and S-wave velocity models. The initial models are 1D linearly increasing velocity models. The results of elastic NLCG FWI are

shown in Figure 2 b and e. These results were computed after 20 nonlinear conjugate gradient iterations. The elastic Gauss-Newton FWI has iterated 10 times for the outer FWI loop and 40 times for the inner CGLS loop (Figure 2 c and f). The velocity models obtained by elastic Gauss-Newton FWI have high-resolution than the ones obtained by elastic NLCG FWI.

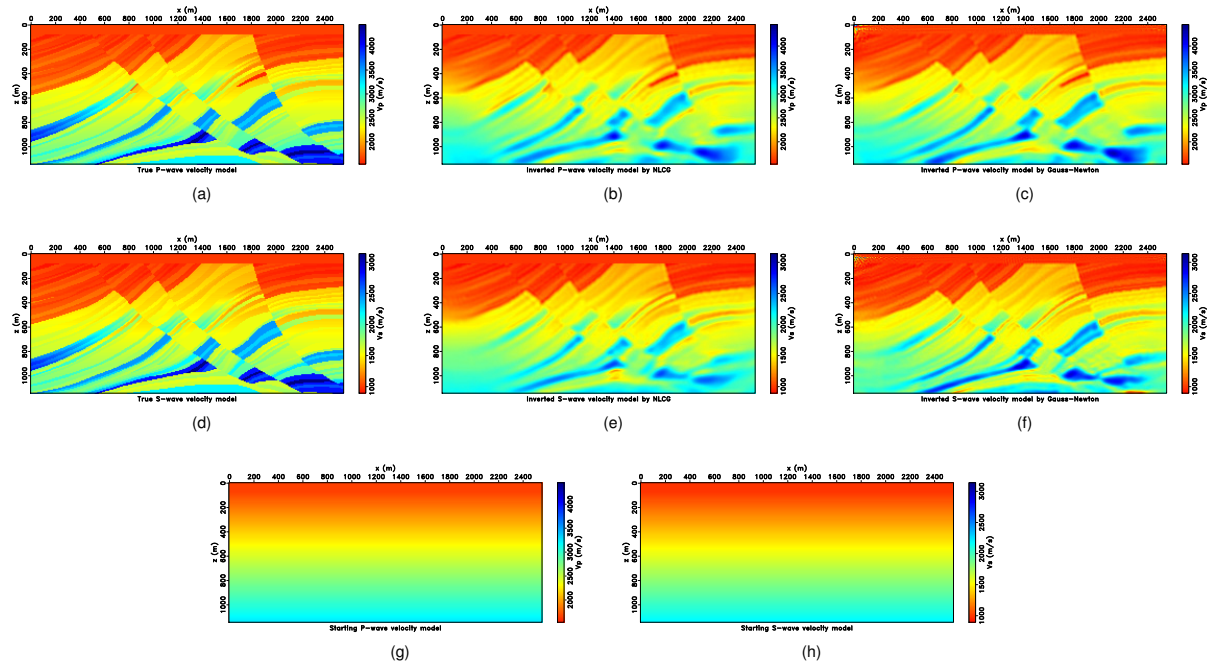

Figure 2: Elastic Marmousi2 model. (a) True P-wave velocity model. (b) Inverted P-wave velocity model by elastic NLCG FWI. (c) Inverted P-wave velocity model by elastic Gauss-Newton FWI. (d) True S-wave velocity model. (e) Inverted S-wave velocity model by elastic NLCG FWI. (f) Inverted S-wave velocity model by elastic Gauss-Newton FWI. (g) Starting P-wave velocity model. (h) Starting S-wave velocity model.

Conclusions

We propose a time-domain matrix-free elastic Gauss-Newton FWI algorithm based on elastic LSRTM algorithm. The proposed algorithm consists of two loops of iterations: the outer Gauss-Newton nonlinear iterations and the inner conjugate gradient least-squares (CGLS) linear iterations. The Gauss-Newton search direction in each outer FWI iteration is computed using the matrix-free CGLS algorithm. We point out that this step is actually equivalent to apply an elastic LSRTM on data residual, with the Jacobian operator as elastic Born modeling operator and the adjoint of Jacobian operator as elastic RTM operator. The CGLS algorithm can be safely used for solving the Gauss-Newton search direction because our discretized numerical versions of elastic Born and RTM operators passed the dot-product test. The inner CGLS linear iterations are preconditioned using the elastic pseudo-Hessian operator. Our algorithm is matrix-free that only requires the forward Jacobian and adjoint Jacobian operator applied “on the fly” to vectors. The operators are applied on vectors efficiently via the adjoint-state method. We use the proposed algorithm to simultaneously invert for P- and S-wave velocities.The proposed elastic Gauss-Newton FWI generates better inverted models than the nonlinear conjugate gradient method based elastic FWI. More importantly, the elastic Gauss-Newton FWI can reduce the crosstalk between P- and S-wave velocity models.

Acknowledgements

We thank the sponsors of the Signal Analysis and Imaging Group (SAIG) at the University of Alberta for financial support. High-performance clustered computational resources were provided by Compute Canada. Figures in this paper were plotted using the Madagascar open-source software package.

REFERENCES

Bunks, C., F. M. Saleck, S. Zaleski, and G. Chavent, 1995, Multiscale seismic waveform inversion: Geophysics, **60**, 1457–1473.

Chen, K., and M. Sacchi, 2017a, Elastic least-squares reverse time migration via linearized elastic full-waveform inversion with pseudo-hessian preconditioning: 87th Annual International Meeting, SEG, Expanded Abstracts, 4364–4369.

Chen, K., and M. D. Sacchi, 2017b, Elastic least-squares reverse time migration via linearized elastic full-waveform inversion with pseudo-Hessian preconditioning: Geophysics, **82**, S341–S358.

Claerbout, J. F., 1992, Earth soundings analysis: Processing versus inversion: Blackwell Scientific Publications Cambridge, Massachusetts, USA, **6**.

Epanomeritakis, I., V. Akcelik, O. Ghattas, and J. Bielak, 2008, A Newton-CG method for large-scale three-dimensional elastic full-waveform seismic inversion: Inverse Problems, **24**, 034015.

Kohn, D., D. De Nil, A. Kurzmann, A. Przebindowska, and T. Bohlen, 2012, On the influence of model parametrization in elastic full waveform tomography: Geophysical Journal International, **191**, 325–345.

Lions, J. L., 1971, Optimal control of systems governed by partial differential equations: Springer Berlin Heidelberg.

Mora, P., 1987, Nonlinear two-dimensional elastic inversion of multioffset seismic data: Geophysics, **52**, 1211–1228.

Paige, C. C., and M. A. Saunders, 1982, LSQR: An algorithm for sparse linear equations and sparse least squares: ACM Trans. Math. Softw., **8**, 43–71.

Pan, W., K. A. Innanen, G. F. Margrave, M. C. Fehler, X. Fang, and J. Li, 2016, Estimation of elastic constants for HTI media using Gauss-Newton and full-Newton multiparameter full-waveform inversion: Geophysics, **81**, R275–R291.

Sheen, D.-H., K. Tuncay, C.-E. Baag, and P. J. Ortoleva, 2006, Time domain Gauss-Newton seismic waveform inversion in elastic media: Geophysical Journal International, **167**, 1373–1384.

Shin, C., S. Jang, and D.-J. Min, 2001, Improved amplitude preservation for prestack depth migration by inverse scattering theory: Geophysical Prospecting, **49**, 592–606.

Tarantola, A., 1984, Inversion of seismic reflection data in the acoustic approximation: Geophysics, **49**, 1259–1266.

——, 1986, A strategy for nonlinear elastic inversion of seismic reflection data: Geophysics, **51**, 1893–1903.